

The influence of Composite Lay-Up and the Shape of the Closed Section on the Stability of the Structure

Błażej Czajka¹, Patryk Różyło^{1*}

¹ Mechanical Engineering Faculty, Lublin University of Technology, ul. Nadbystrzycka 36, 20-618 Lublin, Poland

* Corresponding author's e-mail: p.rozylo@pollub.pl

ABSTRACT

Stability tests of a thin-walled composite structure with a closed section are presented in this paper. The purpose of this paper is to conduct preliminary studies in the context of numerical simulations of critical and slightly post-buckling states. The tests were conducted based only on numerical simulations by the finite element method. Numerical simulations were conducted using ABAQUS software, which allowed to determine the values of critical loads and their corresponding buckling forms. The influence of layer arrangement on the stability of the structure was studied. Carbon-epoxy laminate (CEL) was used in the tests. It is shown that there are composite lay-ups that show more than 1.3 times higher stiffness than the other cases. The paper demonstrates the dependence of the influence of the arrangement of layers on the stability of the structure, which will provide the basis for planned experimental studies (the results require experimental verification, which will be carried out in subsequent studies).

Keywords: buckling, composite closed-section profiles, critical load, FEM.

INTRODUCTION

The continuous increase in the use of thin-walled composite sections (especially carbon-epoxy composites) as responsible load-bearing elements creates a need for further investigation. An important issue for thin-walled structures due to their use to carry loads is stability commonly referred as buckling [1–4]. In the paper [2], the issues of stability and failure of compressive thin-walled structures with open cross-sections were presented in a thorough manner, which provides, in a sense, the basis for the research presented in this paper.

Buckling phenomenon is particularly often observed for thin-walled sections. The effects of external loads such as compression (axial or non-axial) can throw the structure out of equilibrium state. Stability is the ability of a mechanical structure to return independently to its equilibrium state and is highly desirable for structural elements [5–9]. In the paper [8], stability issues of thin-walled structures with open sections are

presented in a thorough manner, with the main focus on the determination of critical loads, using numerical simulations and experimental approximation methods. The initial state of axial compression called the membrane state causes only compression of the walls of the structure. Then a critical state is reached where stability is lost and the form of deformation of the structure changes. After that, the structure goes into a post-buckling state where the deformation progresses with the increase of load [10–14]. The paper [11] presents in particular the phenomenon of failure of compressed composite structures with open sections in a detailed form, using advanced numerical models and independently conducted experimental tests (including the method of acoustic emission).

Most of the scientific papers devoted to the loss of stability of composite thin-walled structures focus on plates and profiles with open cross-sections [15–19]. The present work is dedicated to the simulation of loss of stability phenomenon for structures with closed cross-sections. These

structures exhibit higher stiffness and thus undergo loss of stability at higher loads. The high importance for engineering applications of research on open cross-section profiles provided a reason to start research with closed cross-sections. Thin-walled composite structures with closed cross-sections are also used in industry but a comprehensive analysis of their buckling phenomenon is still lacking [20, 21]. The present work is a continuation of the preliminary research carried out within the project No. 2021/41/B/ST8/00148 financed by the National Science Centre, Poland, the results of which are also shown in the previous work [22].

The subject of study

In this paper, thin-walled composite columns with rectangular cross-sections were the subject of

study. Specimens with two different geometric dimensions of the cross-section (G1 – 30×50 mm; G2 – 20×60 mm) - were prepared (Fig. 1).

The structures consisted of 8 layers of composite material arranged symmetrically to the center plane of the laminate. The used plies had a thickness of 0.1 mm each which translated into a total laminate thickness of 0.8 mm. Four different ply configurations were investigated:

- P1 – [0/45/-45/90]_s,
- P2 – [0/90/0/90]_s,
- P3 – [45/-45/90/0]_s,
- P4 – [90/-45/45/0]_s.

Carbon-epoxy laminate (CEL) was used in the test specimens. Its mechanical and strength properties were applied as presented in Table 1 [11]. In this paper, only numerical analysis of axially compressed thin-walled composite structures was carried out.

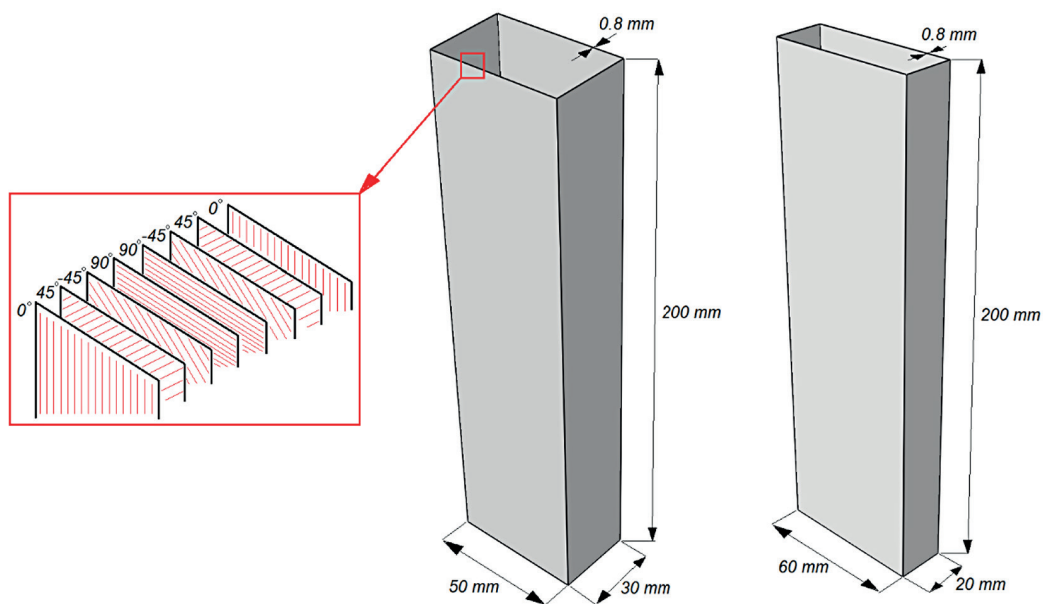


Fig. 1. Geometrical parameters of the tested samples

Table 1. Mechanical and strength properties of carbon-epoxy laminate

Mechanical properties			
Young's modulus	E_1	130710	[MPa]
	E_2	6360	
Kirchhoff modulus	G_{12}	4180	
Poisson's coefficient	ν_{12}	0.32	-
Strength properties			
Tensile strength	$F_{T1} (0^\circ)$	1867.2	[MPa]
Compressive strength	$F_{C1} (0^\circ)$	1531	
Tensile strength	$F_{T2} (90^\circ)$	25.97	
Compressive strength	$F_{C2} (90^\circ)$	214	
Shear strength	F_{12}	100.15	

NUMERICAL SIMULATIONS

The study was conducted using numerical simulation in Abaqus software based on the finite element method [23, 24]. The numerical simulation was based on solving an eigenproblem to determine the stability of the tested element. The solution was based on the minimum potential energy criterion. Mathematical notation of the loss of stability phenomenon is possible due to the equation:

$$K + \lambda H = 0 \quad (1)$$

where: K – stiffness matrix, λ – critical variable (bifurcation load in this case), H – geometric stiffness matrix.

Several assumptions had to be made to solve the loss of stability phenomenon. During the preparation of the numerical model, two non-deformable plates were added as supports for the thin-walled columns. The arrangement of the elements together with the boundary conditions are shown in Figure 2. The boundary conditions were added at specially created reference points (RP) connected to the plates. The first plate was fully fixed with no movement in any direction. The other one had the ability to move only in the direction along the height of the test specimen (following the Z-axis in Figure 2). Contact interactions in the normal and tangential directions were created between the specimens and the supports. A friction coefficient of 0.2 was used.

Shell finite elements were used to discretize the model. S4R elements with a linear shape

function and reduced integration were used for the samples. Each of the 2000 created elements had 4 computational nodes. Each node had 3 translational and 3 rotational degrees of freedom. A global mesh density of 4 mm was used for the composite columns. The discrete model including composite structure G1 was characterized by having 7144 nodes and 6900 finite elements, while the second model including structure G2 was characterized by having 6442 nodes and 6200 finite elements.

The main focus of this paper was on the buckling phenomenon of thin-walled composite structures with rectangular cross-sections. The influence of the ratio of cross-sectional dimensions and the arrangement of layers on the stability of tested samples was examined. This paper is based solely on the results of numerical simulations, which in the future will be validated by experimental research.

Moreover, in addition to the critical state analysis (linear stability analysis of the structure), nonlinear stability analysis of the structure (in the critical load range) was performed in this paper. Simulations of nonlinear stability analysis were based on the incremental-iterative Newton-Raphson method. This allowed the determination of the equilibrium paths of the structure, enabling a better assessment of the critical state.

$$F^N(u^M) = 0 \quad (2)$$

where: F^N constitutes the force component conjugate to the N^{th} variable in the problem and u^M is the value of the M^{th} variable.

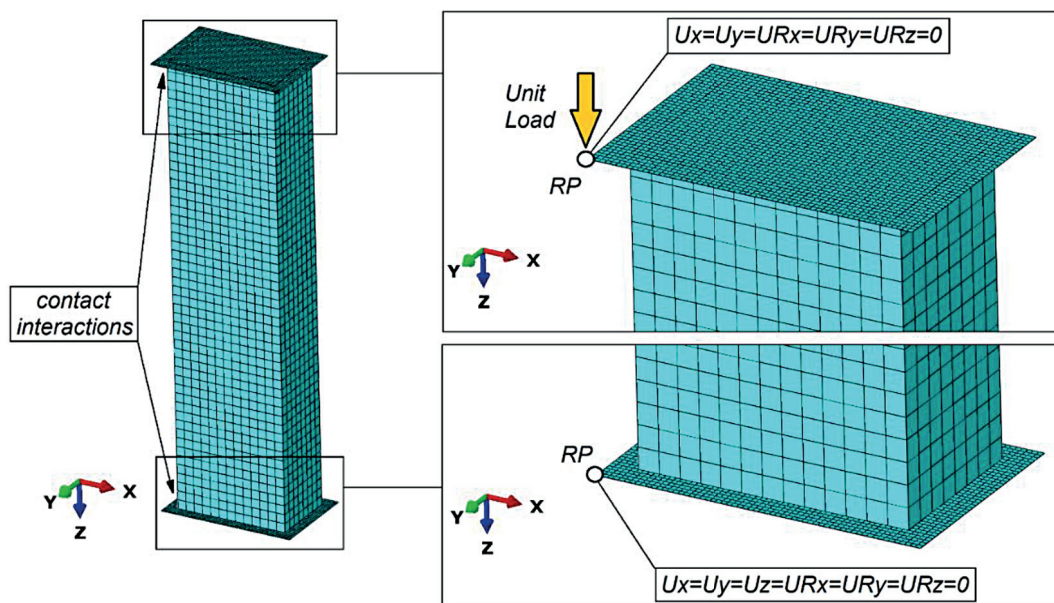


Fig. 2. Discrete model with boundary conditions

Numerical simulation generally uses Newton’s method as a numerical technique for solving the nonlinear equilibrium equations. The motivation for this choice is the convergence rate obtained by using Newton’s method compared to the convergence rates exhibited by other similar methods (modified Newton or quasi-Newton methods). Assume that, after an iteration i , an approximation u_i^M , to the solution has been obtained. Let c_{i+1}^M be the difference between this solution and the exact solution to the discrete equilibrium equation (2). Regarding the above:

$$F^N(u_i^M + c_{i+1}^M) = 0 \tag{3}$$

Expanding the left-hand side of this equation (Taylor series) about the approximate solution then gives:

$$F^N(u_i^M) + \frac{\partial F^N}{\partial u^P}(u_i^M)c_{i+1}^P + \frac{\partial^2 F^N}{\partial u^P \partial u^Q}(u_i^M)c_{i+1}^P c_{i+1}^Q + \dots = 0 \tag{4}$$

In the case of u_i^M is a close approximation to the solution, the magnitude of each c_{i+1}^M will be small, and so all but the first two terms above can be neglected giving a linear system of equations:

$$K_i^{NP} c_{i+1}^P = -F_i^N, \quad K_i^{NP} = \frac{\partial F^N}{\partial u^P}(u_i^M), \tag{5}$$

$$F_i^N = F^N(u_i^M)$$

The next approximation to the solution is then:

$$u_{i+1}^M = u_i^M + c_{i+1}^M \tag{6}$$

and the iteration continues. The above relationships describe the algorithm of the method used for the nonlinear problem.

RESULTS

The achieved results of the numerical analyses are presented in this part. The obtained buckling form and the related critical load were analysed. The results are presented based on the first buckling form of the structure. The results for 4 different lay-ups for each of the 2 tested cross-section geometries (G1 – 30×50 mm; G2 – 20×60 mm) are compared.

For configuration P1 – [0/45/-45/90]_s, similar buckling forms were observed for both tested specimen geometries (Fig. 3.). These are characterised by the occurrence of 3 half-waves on each wall of the composite column located in the height direction of the specimens. However, for the G1 geometry the critical load was significantly higher at $P_{cr[P1G1]} = 6052.1$ N, while for the G2 geometry it was $P_{cr[P1G2]} = 4353.6$ N.

Specimens made in P2 layer configuration - [0/90/0/90]_s (Fig. 4.) behave differently. For the G1 geometry, 4 half-waves are visible, while for the G2 configuration only 3 half-waves very similar to those for the P1 layer configuration. It is

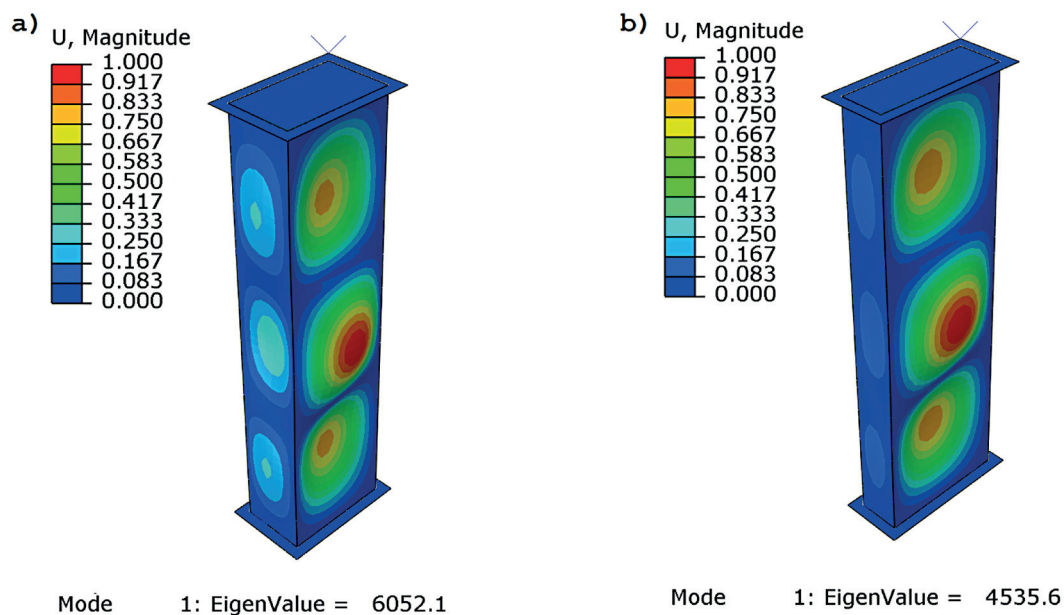


Fig. 3. Simulation results for P1 configuration: a) G1 geometry, b) G2 geometry

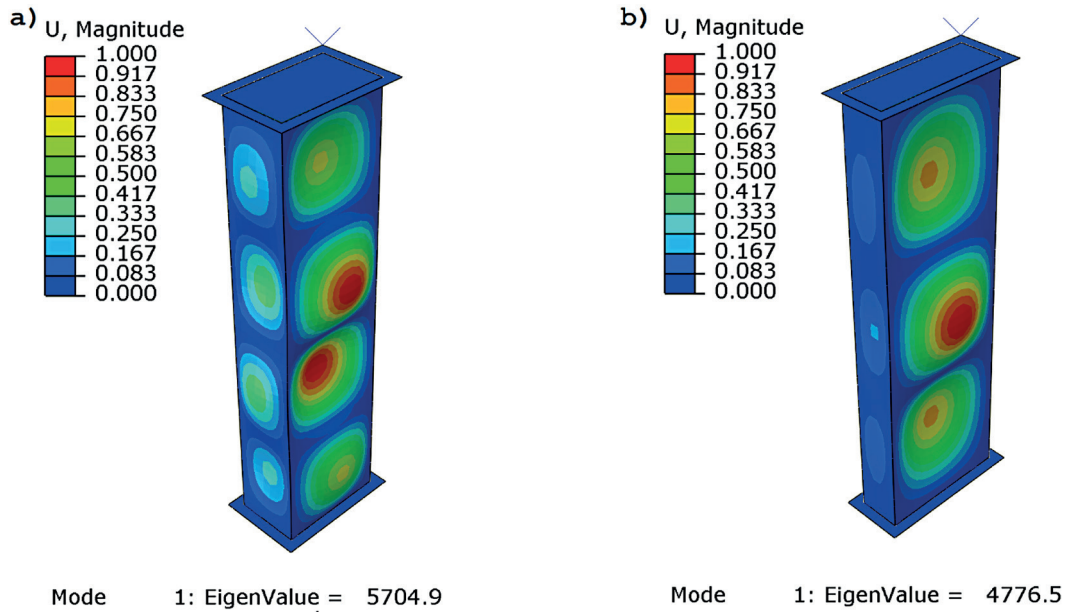


Fig. 4. Results - layer arrangement P2: a) geometry G1, b) geometry G2

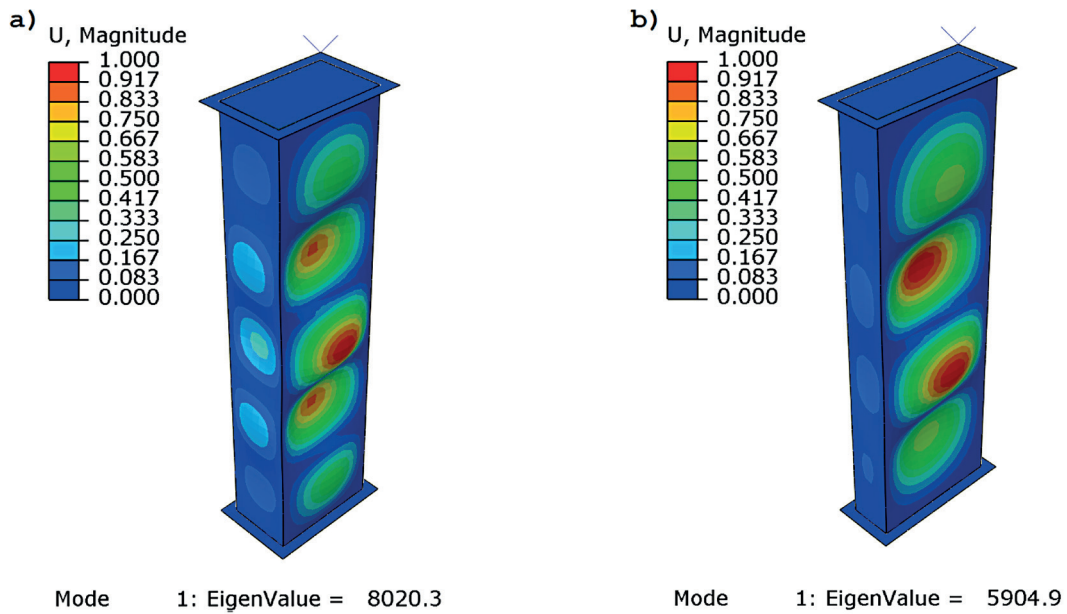


Fig. 5. Results for configuration P3: a) cross-section G1, b) cross-section G2

important to emphasize that the difference of critical loads for different cross-sections was smaller than for the previous layout. The critical load in this layer arrangement was the lowest for the G1 geometry and reached $P_{cr[P2G1]} = 5704.9$ N. For G2 it was $P_{cr[P2G2]} = 4776.5$ N.

The P3 - $[45/-45/90/0]_s$ layer configuration resulted in the highest critical load values for both cross-sections of the specimens. For geometry G1 the critical load was $P_{cr[P3G1]} = 8020.3$ N, and for G2 only $P_{cr[P3G2]} = 5904.9$ N. The first geometry was characterised by the occurrence of 5

half-waves, while the second was characterised by the occurrence of 4 half-waves (Fig. 5.).

The last of the analysed layout P4 - $[90/-45/45/0]_s$ resulted in the lowest critical load for geometry G2 with $P_{cr[P4G2]} = 4461.6$ N. The critical load for the G1 geometry was higher with $P_{cr[P4G1]} = 5910.6$ N. For both geometries, the buckling form was similar and 6 half-waves occurred on the wider wall (Fig. 6).

The results obtained show that both investigated parameters of the specimens (layer configuration and cross-section geometry) have a

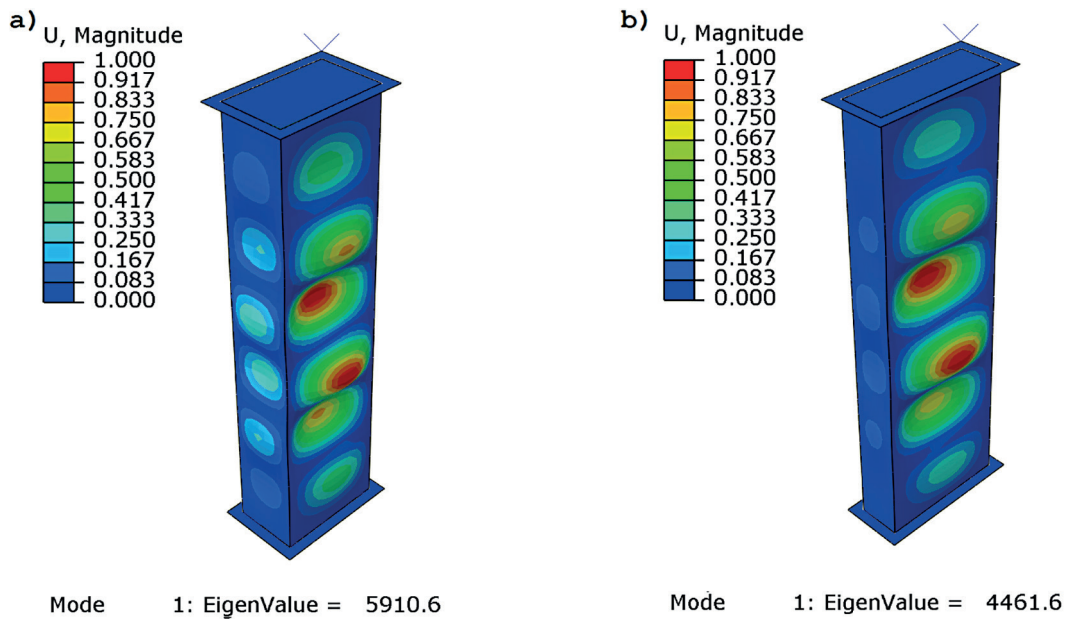


Fig. 6. Simulation results for P4: a) G1 geometry, b) G2 geometry

Table 2. Critical load values

P	P _{cr} [N]		
	G1 – 30 mm × 50 mm	G2 – 20 mm × 60 mm	G1/G2
P1 – [0/-45/45/90] _s	6052.1	4535.6	1.33
P2 – [0/90/0/90] _s	5704.9	4776.5	1.19
P3 – [45/-45/90/0] _s	8020.3	5904.9	1.36
P4 – [90/-45/45/0] _s	5910.6	4461.6	1.32

significant influence on the buckling behaviour of the structure. They cause a change in both the buckling form and the critical load value corresponding to the buckling of the structure. Changing the arrangement of the layers from P1 to P4 caused an increase in the amount of half-waves (or remaining the same number for P1 and P2 in the G2 geometry). However, this did not affect the continuous increase of the critical load values. Moreover, the maximum deformations for each of the tested specimens were at the middle part of the profile height, regardless of the layer arrangement and cross-section geometry.

The P3 configuration showed the highest structural stiffness for both geometries which corresponds to the results for the square cross-section presented in a previous paper [22]. This confirms that arranging the outer composite layer at an angle of 45 and the next at -45 degrees results in the highest structural stiffness. The lowest critical load values were observed for different arrangements of the composite layers. The obtained critical load results are summarised in Table 2.

The highest critical load value observed for geometry G1 ($P_{cr [P3G1]} = 8020.3$ N) was as much as 1.36 times higher than for geometry G2 ($P_{cr [P3G2]} = 5904.9$ N). For each of the tested layups, the critical loads were higher for the G1 cross-section. Previous studies [22] showed significantly higher critical load values for structures with a square cross-section for each layup. Based on these results, a very important conclusion regarding composite profiles with a rectangular cross-section can be derived. If the cross-section is more nearly square (the ratio of the sides of a rectangle is closer to 1), the stiffness of a structure made of a composite material (laminate) is higher.

The results significantly contribute to the development of knowledge concerning the design of structures based on thin-walled composite structures with closed sections. However, they require experiments to confirm the results obtained in simulations. The conducted research is a foundation for conducting further studies regarding non-linear stability and failure analysis of composite structures with closed sections.

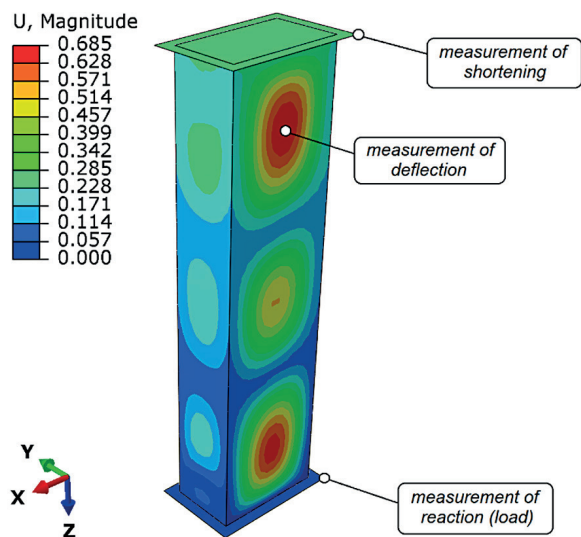


Fig. 7. Measurement of nonlinear stability analysis parameters

Within the framework of numerical investigations, the non-linear stability of the structure was additionally investigated, in order to better represent the behaviour of the structure subjected to critical loads. For this purpose, based on the nonlinear analysis of structural stability, the tested columns were subjected to loads equivalent to critical loads – which allowed the determination of shortening and deflection of thin-walled

structures. Figure 7 shows an example of the points at which the necessary parameters were measured during the numerical simulation (shortening – along the Z axis, deflection – along the Y axis, and reaction (load) measurements).

A measurable result of the conducted research was the determination of the equilibrium paths of the structures, where the research was conducted up to the value of the load, corresponding to the critical load for each of the thin-walled structures.

On the basis of the preliminary analysis of the nonlinear stability of the structure, it was observed that the structure with the P3 arrangement of layers was characterized by the highest shortening (0.32 mm – G1, 0.24 mm – G2), while the structure with the P2 arrangement of layers was characterized by the lowest (0.16 mm – G1, 0.15 mm – G2). The maximum shortening registered for the P3 arrangement of layers, was 1.33 times higher for the G1 profile relative to G2. It was also estimated that the highest deflection was observed in the structure with the P1 arrangement of layers (0.66 mm – G1, 0.69 mm – G2), while the lowest in the structure with the P4 arrangement of layers (0.38 mm – G1, 0.41 mm – G2). The maximum deflection registered for the P1 arrangement of layers, was 1.05 times higher for the G2 profile relative to G1.

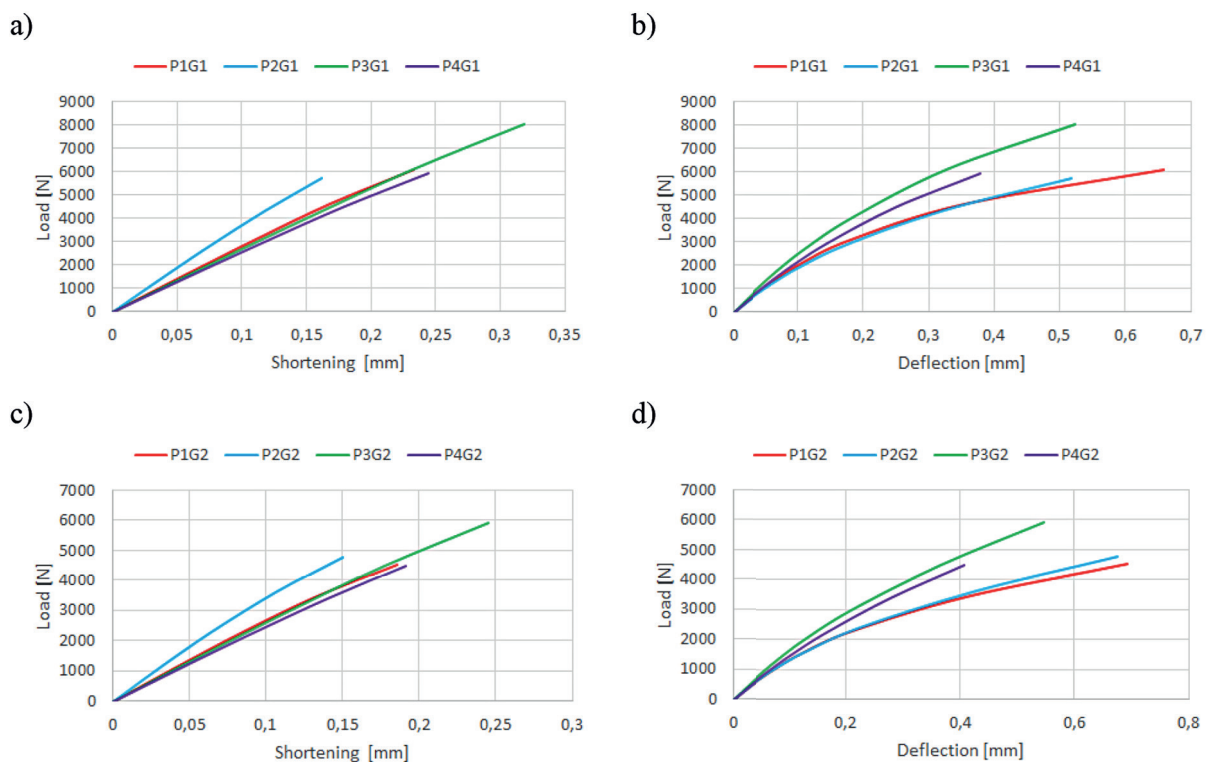


Fig. 8. Equilibrium paths of the structure: a) load-shortening of G1 profile, b) load-deflection of G1 profile, c) load-shortening of G2 profile, d) load-deflection of G2 profile

In addition, it was observed that the level of maximum registered shortening is slightly higher for profiles with G1 cross-section than for profiles with G2 cross-section. The opposite situation occurs in the case of the maximum registered deflection, as the maximum deflection for profiles with cross-section G2, is higher than for profiles G1. Both dependencies were observed regardless of the arrangement of the composite layers.

In this paper, an in-depth analysis of the non-linear stability condition of the structure was not conducted, as this will be the subject of further research, after experimental testing.

CONCLUSIONS

The numerical analysis of buckling of thin-walled composite structures with rectangular cross-sections allowed to make a preliminary assessment of stability. The research carried out resulted in the following conclusions: the solution of the linear eigenproblem by using the FEM allows to determine the critical state for composite sections with rectangular cross-sections. The arrangement of the layers has a significant influence on the form of buckling and the critical load value. Specimens with layers arranged at angles of ± 45 degrees on the outer layers are characterised by the highest stiffness. The geometric dimensions of the cross-section change the form of buckling and the critical load value. If the cross-section is closer to the square the critical load value is higher [22].

Acknowledgments

The research was conducted under project No. 2021/41/B/ST8/00148 financed by the National Science Centre, Poland.

REFERENCES

1. Teter A., Kolakowski Z. Coupled dynamic buckling of thin-walled composite columns with open cross-sections. *Compos. Struct.* 2013; 95: 28–34.
2. Rozylo P. Failure analysis of thin-walled composite structures using independent advanced damage models. *Compos. Struct.* 2021; 262: 113598.
3. Paszkiewicz M., Kubiak T. Selected problems concerning determination of the buckling load of channel section beams and columns. *Thin Walled Struct.* 2015; 93: 112–121.
4. Singer J., Arbocz J., Weller T. *Buckling Experiments: Experimental Methods in Buckling of Thin-Walled Structure: Basic Concepts, Columns, Beams, and Plates*; John Wiley and Sons Inc.: New York, NY, USA 2000, 1.
5. Banat D., Mania R.J. Failure assessment of thin-walled FML profiles during buckling and postbuckling response. *Compos B Eng.* 2017; 112: 278–289.
6. Turvey G.J., Zhang Y. A computational and experimental analysis of the buckling, postbuckling and initial failure of pultruded GRP columns. *Compos. Struct.* 2006; 84: 1527–1537.
7. Teter A., Kolakowski Z. Buckling of thin-walled composite structures with intermediate
8. Rozylo P., Teter A., Debski H., Wysmulski P., Falkowicz K. Experimental and Numerical Study of Buckling of Composite Profiles with Open Cross Section under Axial Compression. *Appl. Compos. Mater.* 2017; 24: 1251–1264.
9. Ascione F. Influence of initial geometric imperfections in the lateral buckling problem of thin walled pultruded GFRP I-profiles. *Compos. Struct.* 2014; 112: 85–99.
10. Ribeiro M.L., Vandepitte D., Tita V. Damage model and progressive failure analyses for filament wound composite laminates. *Appl. Compos. Mater.* 2013; 20: 975–992.
11. Rozylo P. Stability and failure of compressed thin-walled composite columns using experimental tests and advanced numerical damage models. *Int J Numer Methods Eng.* 2021; 122: 5076–5099.
12. Kolanu N.R., Raju G., Ramji M. A unified numerical approach for the simulation of intra and inter laminar damage evolution in stiffened CFRP panels under compression. *Compos. B. Eng.* 2020; 190: 107931.
13. Falkowicz K., Debski H., Wysmulski P., Rozylo P. The behaviour of compressed plate with a central cut-out, made of composite in an asymmetrical arrangement of layers. *Compos. Struct.* 2019; 214: 406–413.
14. Li W., Cai H., Li C., Wang K., Fang L. Progressive failure of laminated composites with a hole under compressive loading based on micro-mechanics. *Adv. Compos. Mater.* 2014; 23: 477–490.
15. Dębski H., Różyło P., Wysmulski P., Falkowicz K., Ferdynus M. Experimental study on the effect of eccentric compressive load on the stability and load-carrying capacity of thin-walled composite profiles, *Compos. B. Eng.* 2021; 190: 109346.
16. Dębski H., Kubiak T., Teter A. Experimental investigation of channel-section composite profiles behavior with various sequences of plies subjected to static compression. *Thin-Walled Struct.* 2013; 71: 147–154.

17. Wael F. Ragheb. Local buckling analysis of pultruded FRP structural shapes subjected to eccentric compression. *Thin Walled Struct.* 2010; 48: 709–717.
18. Nunes F., Correia M., Correia J.R., Silvestre N., Moreira A. Experimental and numerical study on the structural behaviour of eccentrically loaded GFRP columns. *Thin Walled Struct.* 2013; 72: 175–187.
19. Kołakowski Z., Teter A. Load carrying capacity of functionally graded columns with open cross-sections under static compression, *Compos. Struct.* 2015; 129: 1–7
20. Drożdźiel M., Podolak P., Czapski P., Zgórnjak P., Jakubczak P. Failure analysis of GFRP columns subjected to axial compression manufactured under various curing-process conditions. *Compos. Struct.* 2021; 262: 113342
21. Urbaniak M., Świniarski J., Czapski P., Kubiak T. Experimental investigations of thin-walled GFRP beams subjected to pure bending. *Thin-Walled Struct.* 2016; 107: 397–404.
22. Rozyło P., Debski H. The Influence of Composite Lay-Up on the Stability of a Structure with Closed Section. *Adv. Sci. Technol. Res. J.* 2022; 16(1): 260–265.
23. Grzejda R. FE-modelling of a contact layer between elements joined in preloaded bolted connections for the operational condition. *Adv. Sci. Technol. Res. J.* 2014; 8(24): 19–23.
24. Grzejda R. Finite element modelling of the contact of elements preloaded with a bolt and externally loaded with any force. *Journal of Computational and Applied Mathematics* 2021, 393, 113534.